Research Article

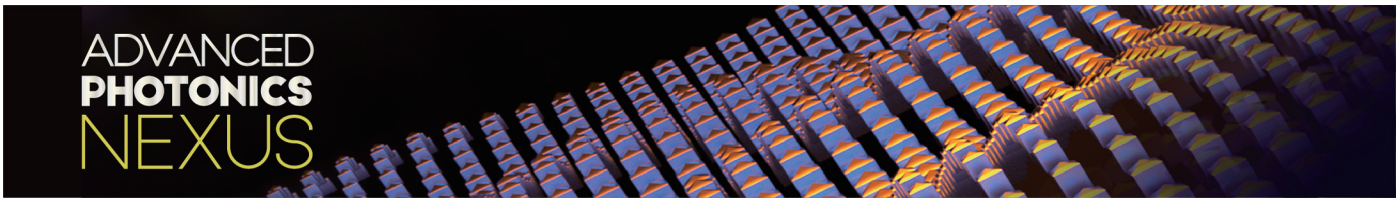


# Multiphoton path-polarization entanglement through a single gradient metasurface

Qi Liu,[a,b] Xuan Liu,[c] Yu Tian,[a,b] Zhaohua Tian,[a] Guixin Li,[d] Xi-Feng Ren,[e,f] Qihuang Gong,[a,b,f,g,h] and Ying Gu[a,b,f,g,h,*]
[a]Peking University, State Key Laboratory for Mesoscopic Physics, Department of Physics, Beijing, China
[b]Peking University, Frontiers Science Center for Nano-optoelectronics and Collaborative Innovation Center of Quantum Matter and Beijing Academy of Quantum Information Sciences, Beijing, China
[c]Beijing University of Technology, Institute of Laser Engineering, Faculty of Materials and Manufacturing, Beijing, China
[d]Southern University of Science and Technology, Department of Materials Science and Engineering, Shenzhen, China
[e]University of Science and Technology of China, CAS Key Laboratory of Quantum Information, Hefei, China
[f]Hefei National Laboratory, Hefei, China
[g]Shanxi University, Collaborative Innovation Center of Extreme Optics, Taiyuan, China
[h]Peking University Yangtze Delta Institute of Optoelectronics, Nantong, China

**Abstract.** Multiphoton entanglement with high information capacity plays an essential role in quantum information processing. The appearance of parallel beam splitting (BS) in a gradient metasurface provides the chance to prepare the multiphoton entanglement in one step. Here, we use a single metasurface to construct multiphoton path-polarization entanglement. Based on the parallel BS property, entanglement among $N$ unentangled photons is created after they pass through a gradient metasurface. Also, with this ability, entanglement fusion among several pairs of entangled photons is set up, which can greatly enlarge the entanglement dimension. These theoretical results pave the way for manipulating metasurface-based multiphoton entanglement, which holds great promise for ultracompact on-chip quantum information processing.

Keywords: quantum entanglement; gradient metasurface; quantum beam splitting.

Received Sep. 19, 2024; revised manuscript received Nov. 19, 2024; accepted for publication Jan. 9, 2025; published online Feb. 13, 2025.



[DOI: 10.1117/1.APN.4.2.026002]

## 1 Introduction

Multiphoton entanglement with high information capacity plays an essential role in quantum information processing.[1,2] Currently, there are two main ways to create multiphoton entanglement. The first one is based on quantum nonlinear optical processes, such as spontaneous parametric downconversion (SPDC)[3] and spontaneous four-wave mixing (SFWM),[4] which is convenient for generating entangled photon pairs but with low efficiency. To obtain multiphoton entanglement, several coherently driving SPDC/SFWM processes are required,[5–8] where the generating efficiency decreases rapidly as the number of photons increases. The second one relies on a linear beam splitting (BS) process with quantum interference.[9] Integrated photonic systems[10,11] utilizing linear BS[12] provide a platform for manipulating multiphoton and high-dimensional entanglement. Also, BS processes can facilitate the fusion of multiple entangled states.[13,14] Nevertheless, the above multiphoton entanglement or entanglement fusion needs a set of beam splitters working simultaneously. The use of too many beam splitters may bring some problems, such as loss and cross talk, which will greatly reduce the success probability in quantum operations. Therefore, achieving the compact generation of multiphoton entanglement remains a challenge for on-chip quantum information processing.

Metasurfaces provide new opportunities for the preparation of entanglement due to their ability to control multiple degrees of freedom of light,[15–20] such as phase distribution, frequency, and polarization. By modulating phase and frequency, the generation of multiphoton entanglement has been demonstrated with nonlinearity-integrated metasurfaces,[21,22] but it still suffers from the issue of low efficiency. Based on various phase

*Address all correspondence to Ying Gu, ygu@pku.edu.cn

gradient designs, metasurfaces with polarization-dependent,[23,24] variable splitting ratios,[25] and multichannel[26] properties are used to realize the BS capabilities. Then, these metasurface-based BSs have led to some entanglement applications, including multi-degree-of-freedom entanglement,[27–29] entangled state reconstruction,[30,31] and multichannel distribution of entanglement.[32] However, most of the above results are limited to two-photon entanglement because only one BS process is used, whereas multiphoton entanglement has not been proposed in metasurfaces with BS functions. Fortunately, it has been found that the BS process on a gradient metasurface is parallelable, i.e., a single metasurface can function as a series of parallel-linked beam splitters.[33] This parallel BS capability enables multibeam interference, so in principle, it is capable of generating multiphoton entanglement on a single metasurface.

Here, utilizing parallel BS property, we demonstrate the multiphoton path-polarization entanglement on a single metasurface. Based on the quantum interference of multiphoton, $N$-photon entanglement is obtained after $N$ unentangled photons pass through a gradient metasurface. Furthermore, different types of $N$-photon entangled states are available through changing path-polarization combinations of incident photons. Also, with parallel BS ability, entanglement fusion among several pairs of entangled photons is realized with a single metasurface, which greatly improves the information capacity of entanglement. By providing a simple and compact way for manipulating multiphoton entanglement on a single metasurface, the results hold promise for ultracompact on-chip quantum information processing.

## 2 Model Setup

Consider a Pancharatnam–Berry phase gradient metasurface composed of lossless dielectric materials (a specific design used in this work can be found in the Supplemental Materials of Ref. 33). When a beam of left circularly polarized (LCP) light is incident, part of the light is deflected into the $+1$'th diffraction order, causing a helicity flip in polarization.[16] The remaining light predominantly stays in the 0'th diffraction order, maintaining its original polarization helicity. Conversely, when right circularly polarized (RCP) light is incident along the previously $+1$ diffraction order, it results in the same output beam path and polarization state as before. This constitutes a closed $2\times 2$ BS process between the LCP 0-order light and the RCP $+1$-order light. Recent studies indicate that within the paraxial approximation, numerous $2\times 2$ BS processes occur as the angle of incidence of the incident beam changes.[33] As shown in Fig. 1(b), considering paths within the same set of diffraction orders, a series of parallel $2\times 2$ BS processes coexist, where adjacent processes share a path but in orthogonal polarization modes. The responses of these $2\times 2$ BS processes constitute a parallel array of beam splitters,[33]

$$\begin{bmatrix} E^{\text{out}}_{R,j+1} \\ E^{\text{out}}_{L,j} \end{bmatrix} = \begin{bmatrix} \cos\Delta & i\sin\Delta \\ i\sin\Delta & \cos\Delta \end{bmatrix} \begin{bmatrix} E^{\text{in}}_{R,j+1} \\ E^{\text{in}}_{L,j} \end{bmatrix}, \tag{1}$$

where the subscript $j(=0,\pm1,\pm2,\cdots)$ represents the diffraction order index (path index), and $|\tan(\Delta)|$ is the splitting ratio of each $2\times 2$ BS process. Such a parallel BS response can be understood with the linking beam splitter model shown in Fig. 1(c). Typically, there are three output beams in paths $j$, $j\pm1$ following the incidence of linearly polarized light on path $j$, with the exception of when $\Delta=\pi/2$. In the latter situation, the output light in path $j$ will vanish, leading to only two output paths, $j\pm1$. When multiple beams are incident together, the output lights corresponding to different inputs overlap in some paths, i.e., the interference effect occurs.

In this work, we mainly study the manipulation of multiphoton entangled states with the above parallel BS principle, as illustrated in Fig. 1(a), assuming that some photons in the initial quantum state occupy certain path modes that take part in parallel BS. Then, we consider the quantum state evolution before and after passing through the metasurface. A single photon occupying path $j$ mode with a certain polarization is denoted by Dirac notation $|A\rangle_j=\hat{a}^\dagger_A(j)|0\rangle$ ($A=L,R,H,$ and $V$), where $\hat{a}_H(j)=[\hat{a}_L(j)+\hat{a}_R(j)]/\sqrt{2}$ and $\hat{a}_V(j)=i[\hat{a}_L(j)-\hat{a}_R(j)]/\sqrt{2}$ are annihilation operators of horizontally and vertically polarized photons, respectively. According to the quantum theory of parallel BS,[33,34] the evolution of the quantum mode $\hat{a}^\dagger_A(j)$ is given by the Heisenberg equation of motion,

$$i\hbar\frac{\partial}{\partial t}\hat{a}^\dagger_A(j)=[\hat{a}^\dagger_A(j),\hat{H}_{\text{eff}}], \tag{2a}$$

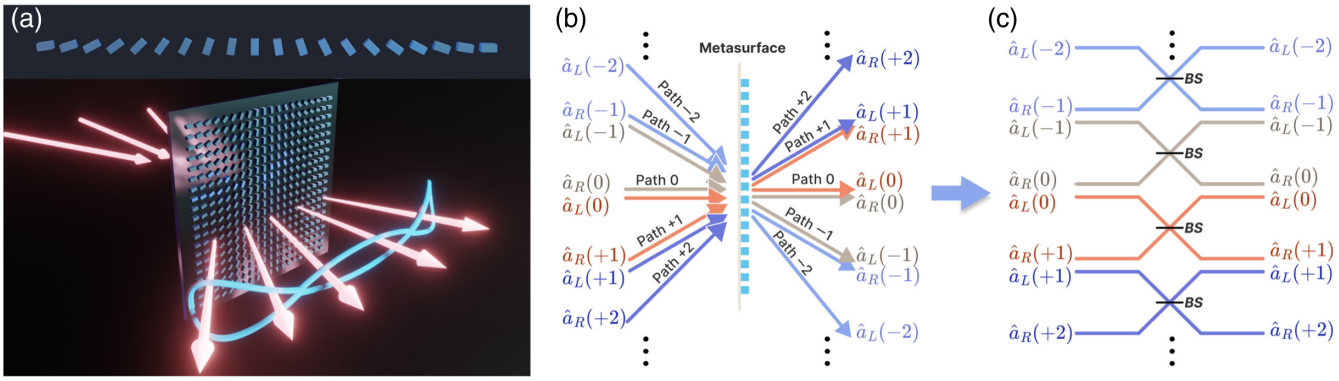


**Fig. 1** (a) Schematic of quantum state manipulation with a parallel BS metasurface. (b) Parallel BS processes on a single metasurface. (c) The model of linked beam splitters for parallel BSs.

$$\hat{H}_{\text{eff}} = -g\hbar \sum_{j=-m}^{m-1} \hat{a}_L^{\dagger}(j)\hat{a}_R(j+1) + h.c., \tag{2b}$$

with $\hat{H}_{\text{eff}}$ being an effective Hamiltonian, and $m$ is related to the number of parallel BS processes on the metasurface. Then, one can obtain the time evolution of the input state $|\psi_{\text{out}}\rangle = \hat{S}(t)|\psi_{\text{in}}\rangle$, where $\hat{S}(t) = \exp(-i\hat{H}_{\text{eff}}t/\hbar)$ is the time evolution operator. The parameter of effective interaction $gt = \Delta$ is associated with the splitting ratio ($|\tan(gt)|$) of BS. Given an input state, certain entangled state components $|\psi_{\text{out}}\rangle_{\text{entangled}}$ may exist in the output state due to quantum interference,

$$|\psi_{\text{out}}\rangle = |\psi_{\text{out}}\rangle_{\text{entangled}} + |\psi_{\text{out}}\rangle_{\text{discard}}. \tag{3}$$

After postselection, the entangled state component $|\psi_{\text{out}}\rangle_{\text{entangled}}$ can be filtered out. Thus, by selecting appropriate input quantum states and postselection, a variety of entanglement manipulations can be achieved, which will be discussed in the following.

## 3 Multiphoton Entanglement with Parallel BS Metasurface

### 3.1 Entangled State Preparation

We first discuss the preparation of two-photon entangled states. As shown in Fig. 2, two LCP photons along paths 0 and +1 are sent into the metasurface, i.e., $|\psi_{\text{in}}\rangle = |L\rangle_0|L\rangle_{+1}$. In this case, at most four modes involve the transformation, so $\hat{H}_{\text{eff}} = -g\hbar\sum_{j=0}^{1}[\hat{a}_L^{\dagger}(j)\hat{a}_R(j+1) + h.c.]$. With the relation $|\psi_{\text{out}}\rangle = \hat{S}(t)|\psi_{\text{in}}\rangle$, $|\psi_{\text{out}}\rangle$ reads

$$\begin{aligned}|\psi_{\text{out}}\rangle = {} & \cos^2\Delta|L\rangle_0|L\rangle_{+1} - \sin^2\Delta|R\rangle_{+2}|R\rangle_{+1} \\ & + i\sin\Delta\cos\Delta(|LR\rangle_{+1} + |L\rangle_0|R\rangle_{+2}).\end{aligned} \tag{4}$$

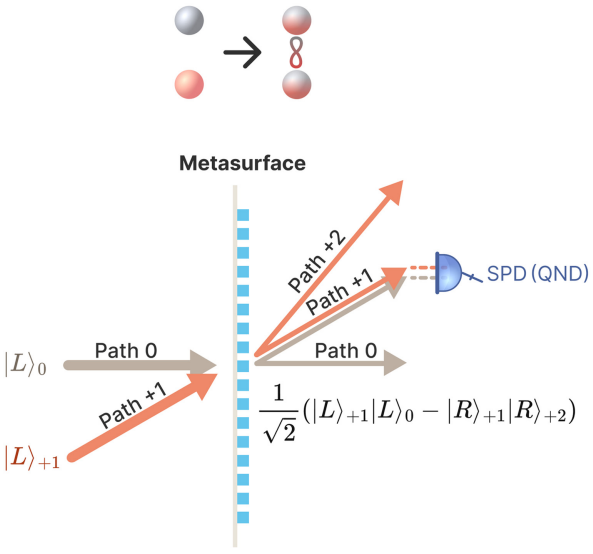


**Fig. 2** Schematic of two-photon entangled state preparation with parallel BS of metasurface. When two LCP photons along paths 0 and +1 are incident to the metasurface, the entangled state $\frac{1}{\sqrt{2}}(|L\rangle_0|L\rangle_{+1} - |R\rangle_{+1}|R\rangle_{+2})$ is prepared after a postselection. Here, SPD is an abbreviation of a single photon detector.

Hereafter, $|\psi_{\text{out}}\rangle_{\text{post}}$ denotes a normalized entangled state after postselection, with the global phase factor being omitted. One can see that the first two terms in Eq. (4), i.e., $|\psi_{\text{out}}\rangle_{\text{post}} = \mathcal{N}(\cos^2\Delta|L\rangle_0|L\rangle_{+1} - \sin^2\Delta|R\rangle_{+2}|R\rangle_{+1})$ ($\mathcal{N}$ is a normalization factor), have a form of entanglement. The entangled component $|\psi_{\text{out}}\rangle_{\text{post}}$ can be postselected if only one photon is detected in path +1, which can be done via quantum nondemolition measurement (QND) of the photon number.[35,36] The success probability of postselection is maximized (50%) when two superposition coefficients have the same amplitude $|\cos^2\Delta| = |-\sin^2\Delta| = 1/2$, such as $\Delta = \pi/4$. Moreover, using the principle of path identity,[8] one can further combine the path $(0, +2)$ into a single path with a circular polarization beam splitter; thus, the postselected state becomes a standard Bell state $(|L\rangle_0|L\rangle_{+1} - |R\rangle_0|R\rangle_{+1})/\sqrt{2}$ that only entangled in a polarization degree of freedom. The postselected entangled state is a consequence of quantum interference, which is contributed by two simultaneous BS processes in the metasurface.

Here, the photons' output paths partially overlap, leading to a distinct quantum interference phenomenon compared with that observed in traditional bulk beam splitters[2,12] and waveguide directional couplers.[10] Unlike these systems, where output paths are the same for each input photon, the interference property in our case endows one output photon with an additional degree of freedom in terms of path. Consequently, the first photon's path and polarization are simultaneously entangled with the polarization of the second photon. Because both polarization and path degrees of freedom participate in entanglement, one photon can be regarded as two qubits. This fact implies an improvement in the dimension of entanglement, which can be understood as a result of the increase in the effective number of qubits. Such a higher-dimensional entanglement with multi-degree-of-freedom is helpful for processing higher-capacity quantum information.[37]

By choosing different input states, one can fabricate several types of two-photon entangled states. In the frame of Fig. 3, if two photons exist, the general form of effective Hamiltonian can be written as $\hat{H}_{\text{eff}} = -g\hbar\sum_{j=-2}^{2}[\hat{a}_L^{\dagger}(j)\hat{a}_R(j+1) + h.c.]$. The splitting parameters are $\Delta = \pi/4$ for Figs. 3(a)–3(c) and $\Delta = \pi/2$ for Fig. 3(d). In Fig. 3(a), if $|\psi_{\text{in}}\rangle = |R\rangle_0|R\rangle_{+1}$, it can be transformed into $|\psi_{\text{out}}\rangle = \hat{S}(t)|\psi_{\text{in}}\rangle$ and then postselected into $|\psi_{\text{out}}\rangle_{\text{post}} = (|R\rangle_0|R\rangle_{+1} - |L\rangle_0|L\rangle_{-1})/\sqrt{2}$, which is achieved by single-photon QND in path 0 with success probabilities of 50%, whereas in Fig. 3(b), $|\psi_{\text{in}}\rangle = |L\rangle_0|R\rangle_{+1}$, then $|\psi_{\text{out}}\rangle_{\text{post}} = (|LL\rangle_0 + |RR\rangle_{+1})/\sqrt{2}$ without any need of the postselection process, i.e., it is postselection-free. In this situation, the output paths of the two photons overlap completely, and the polarization-dependent BS characteristic of the metasurface leads to destructive quantum interference. As a result, two-photon coincident events between paths 0 and +1 are eliminated, deterministically generating the entangled state. Then, for Fig. 3(c), if $|\psi_{\text{in}}\rangle = |L\rangle_{-1}|R\rangle_{+1}$, $|\psi_{\text{out}}\rangle_{\text{post}} = (|L\rangle_0|L\rangle_{-1} + |R\rangle_0|R\rangle_{+1})/\sqrt{2}$, and for Fig. 3(d), $|\psi_{\text{in}}\rangle = |H\rangle_{-1}|H\rangle_{+1}$, then $|\psi_{\text{out}}\rangle_{\text{post}} = (|L\rangle_0|L\rangle_{-2} + |R\rangle_0|R\rangle_{+2})/\sqrt{2}$. In Figs. 3(a) and 3(c), two BSs together are involved in the fabrication process of entanglement, whereas the process in Fig. 3(d) needs four BSs. For any of the above postselection processes, the success probability is 50%. Thus, combining the unique parallel BS property of a metasurface with a suitable postselection together enables various two-photon entangled state preparations.

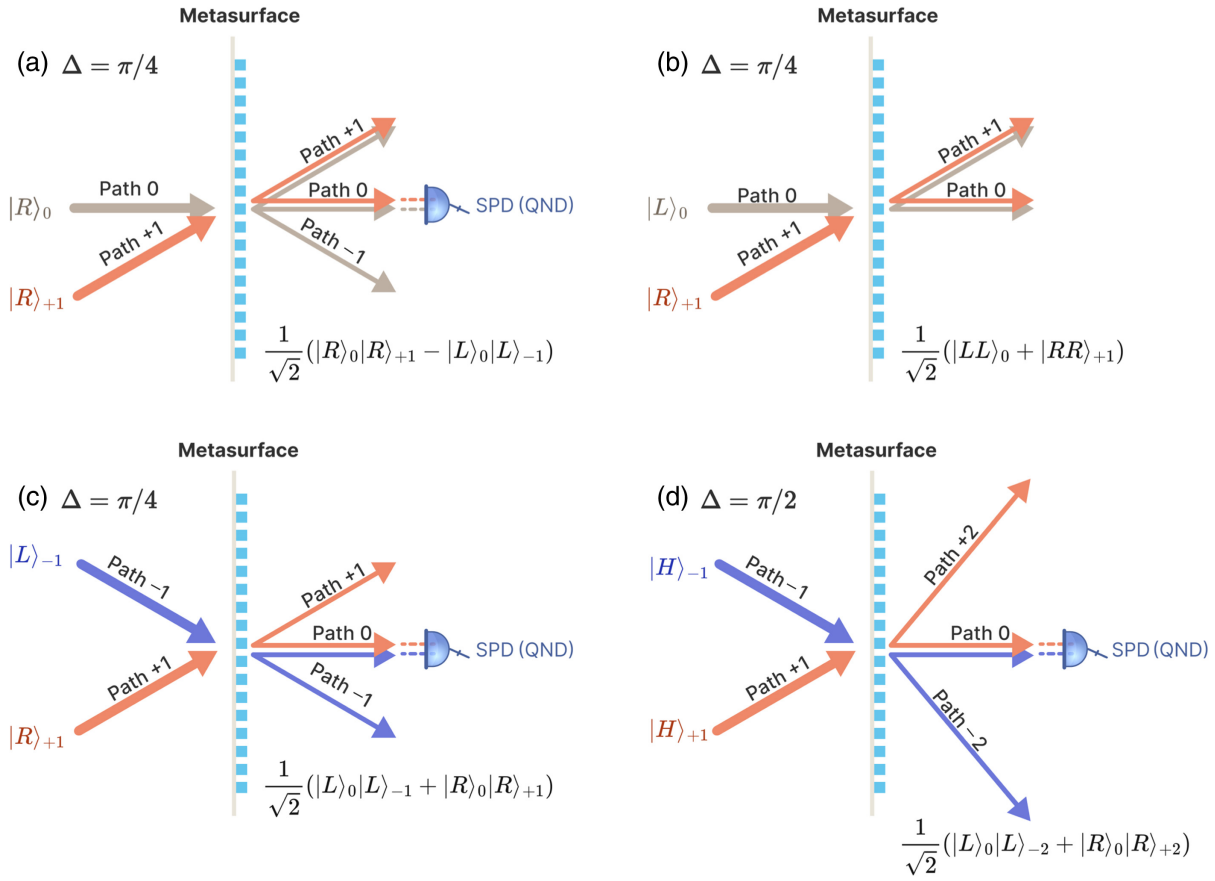


**Fig. 3** Schematic of four kinds of two-photon entangled state preparation with parallel BS of gradient metasurface. (a) $|\psi_{in}\rangle = |R\rangle_0|R\rangle_{+1}$ and $|\psi_{out}\rangle_{post} = (|R\rangle_0|R\rangle_{+1} - |L\rangle_0|L\rangle_{-1})/\sqrt{2}$. (b) $|\psi_{in}\rangle = |L\rangle_0|R\rangle_{+1}$ and $|\psi_{out}\rangle_{post} = (|LL\rangle_0 + |RR\rangle_{+1})/\sqrt{2}$. (c) $|\psi_{in}\rangle = |L\rangle_{-1}|R\rangle_{+1}$ and $|\psi_{out}\rangle_{post} = (|L\rangle_0|L\rangle_{-1} + |R\rangle_0|R\rangle_{+1})/\sqrt{2}$. (d) $|\psi_{in}\rangle = |H\rangle_{-1}|H\rangle_{+1}$ and $|\psi_{out}\rangle_{post} = (|L\rangle_0|L\rangle_{-2} + |R\rangle_0|R\rangle_{+2})/\sqrt{2}$. The splitting parameters are $\Delta = \pi/4$ for panels (a)–(c) and $\Delta = \pi/2$ for panel (d). The postselection with a success probability of 50% is done by single-photon detection in path 0 for panels (a), (c), and (d), whereas for panel (b), the postselection is not required. Here, $|\psi_{out}\rangle_{post}$ has been normalized, with the global phase factor being omitted.

By adding the third photon into an adjacent path, we extend the two-photon case in Fig. 3(a) into the three-photon case in Fig. 4(a). When the input state is $|\psi_{in}\rangle = |R\rangle_{-1}|R\rangle_0|R\rangle_{+1}$, with $\hat{H}_{eff} = -g\hbar\sum_{j=-2}^{0}[\hat{a}_L^\dagger(j)\hat{a}_R(j+1) + h.c.]$ and $|\psi_{out}\rangle = \hat{S}(t)|\psi_{in}\rangle$, $|\psi_{out}\rangle$ reads

$$\begin{aligned}|\psi_{out}\rangle = {} & \cos^3\Delta|R\rangle_{+1}|R\rangle_{-1}|R\rangle_0 - i\sin^3\Delta|L\rangle_{-2}|L\rangle_{-1}|L\rangle_0 \\ & + i\sin\Delta\cos^2\Delta(|LR\rangle_0|R\rangle_{-1} + |LR\rangle_{-1}|R\rangle_{+1} \\ & + |L\rangle_{-2}|R\rangle_0|R\rangle_{+1}) - \cos\Delta\sin^2\Delta(|LR\rangle_0|L\rangle_{-2} \\ & + |LR\rangle_{-1}|L\rangle_0 + |L\rangle_{-2}|L\rangle_{-1}|R\rangle_{+1}).\end{aligned} \tag{5}$$

For the first two components in Eq. (5), $|\psi_{out}\rangle_{post} = \mathcal{N}(\cos^3\Delta|R\rangle_{+1}|R\rangle_{-1}|R\rangle_0 - i\sin^3\Delta|L\rangle_{-2}|L\rangle_{-1}|L\rangle_0)$ ($\mathcal{N}$ is the normalization factor), there exists hybrid entanglement, i.e., the path and polarization of the first photon are entangled with the polarization of the other photons simultaneously. $|\psi_{out}\rangle_{post}$ can be obtained if one photon is postselected in both paths 0 and −1. The success probability to prepare $|\psi_{out}\rangle_{post}$ is maximized to 25% when two superposition coefficients have the same amplitude $|\cos^3\Delta| = |-i\sin^3\Delta|$ as $\Delta = \pi/4$, corresponding to a splitting ratio of 50:50. Similar to the two-photon case, the postselected entanglement comes from three simultaneous BS processes in the metasurface. Also, $|\psi_{out}\rangle_{post}$ can be converted into a GHZ-type maximum entangled state after combining paths $(-2, +1)$ due to path identity,[8] which looks like $(|R\rangle_{+1}|R\rangle_{-1}|R\rangle_0 - i|L\rangle_{+1}|L\rangle_{-1}|L\rangle_0)/\sqrt{2}$.

Just as in the two-photon entanglement process, different setups of parallel BS can fabricate different types of three-photon entangled states. As shown in Fig. 4(b), which is an extension of Fig. 3(d), we input three linearly polarized photons with path indices differing by 2: $|\psi_{in}\rangle = |H\rangle_{-2}|H\rangle_0|H\rangle_{+2}$. Then, the entangled state is obtained under $\Delta = \pi/2$ with a success probability of 1/4, which reads $|\psi_{out}\rangle_{post} = (|L\rangle_{-3}|L\rangle_{-1}|L\rangle_{+1} + |R\rangle_{+3}|R\rangle_{-1}|R\rangle_{+1})/\sqrt{2}$. It is noted that the path and polarization of the first photon are simultaneously entangled with the polarization of the other photons. This is because the path and

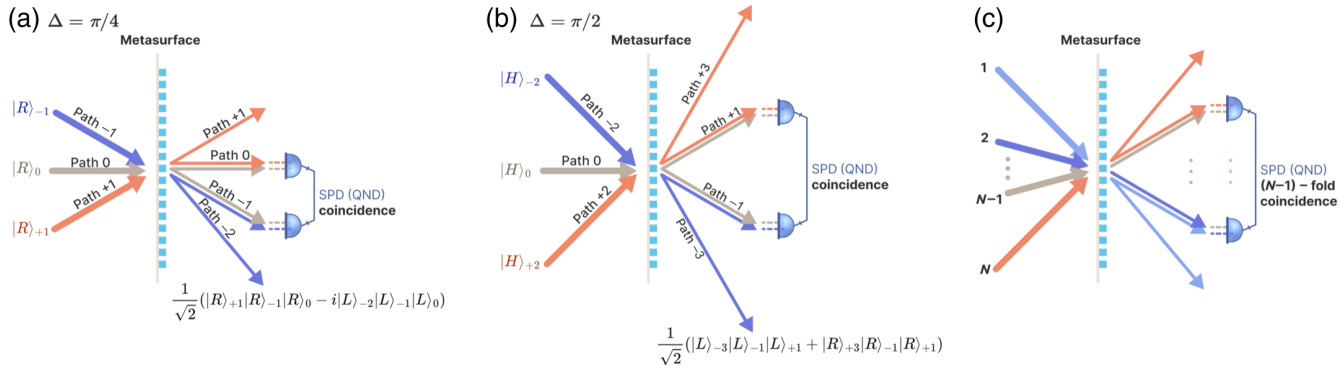


**Fig. 4** Schematic of three-photon entangled state preparations with parallel BS of gradient metasurface. (a) Three-photon entangled state preparation with input state $|\psi_{\text{in}}\rangle = |R\rangle_{-1}|R\rangle_0|R\rangle_{+1}$, which needs single-photon detection coincidence in paths 0 and −1 for postselection. (b) Three-photon entangled state preparation with input state $|\psi_{\text{in}}\rangle = |H\rangle_{-2}|H\rangle_0|H\rangle_{+2}$, which needs single-photon detection coincidence in paths +1 and −1 for postselection. The splitting parameters for panels (a) and (b) are $\Delta = \pi/4$ and $\Delta = \pi/2$, respectively. (c) Extended scheme of Figs. 3(a) or 3(d) for the preparation of an $N$-photon entangled state, which needs $(N-1)$-fold single-photon detection coincidence for postselection.

polarization are locked for the first photon, i.e., the first photon appears in path $-3$ with LCP or appears in path $+3$ with RCP. So, the dimension of entanglement is greatly improved. This postselected state can also be transformed into a GHZ-type entangled state by combining paths $(-3, +3)$ into one single path. Here, six BSs working simultaneously are provided by the single metasurface. Compared with the previous method of three-photon GHZ state preparation,[2] which involved the use of entangled photon pairs and multiple beam splitters, the parallel BS approach facilitated by a single metasurface offers a system that does not require entanglement resources and is highly integrable.

Using the principle of parallel BSs in a gradient metasurface, $N$-photon entanglement can also be prepared. Here, we only give two types of entanglement. As shown in Fig. 4(c), the generation of entanglement is accomplished by simultaneously detecting one photon in each of $(N-1)$ overlapped output paths after inputting $N$ single photons. For the first type, the input state is $|\psi_{\text{in}}\rangle = \otimes_{j=1}^{N} |R\rangle_{m+j} = |R\rangle_{m+1}|R\rangle_{m+2}\cdots|R\rangle_{m+N}$. Then, the metasurface transforms the input state into $|\psi_{\text{out}}\rangle = \hat{S}(t)|\psi_{\text{in}}\rangle$, which reads

$$|\psi_{\text{out}}\rangle = \cos^N\Delta \bigotimes_{j=1}^{N} |R\rangle_{m+j} + i^N \sin^N\Delta \bigotimes_{j=0}^{N-1} |L\rangle_{m+j} + |\psi_{\text{discard}}\rangle, \quad (6)$$

where $|\psi_{\text{discard}}\rangle$ is the discarded component after the postselection. The first two terms in Eq. (6) form an $N$-photon entangled state, which can be postselected by single-photon QND of paths $(m+1, m+2, \ldots, m+N-1)$ with a successful probability $\cos^{2N}\Delta + \sin^{2N}\Delta$. When the two coefficients have the same amplitude, i.e., $\Delta = \pi/4$, the success probability is maximized to $1/2^{N-1}$. Combining paths $(m, m+N)$, the state becomes a GHZ-type polarization-entangled state.

For the second type of $N$-photon entanglement, if the input state is $|\psi_{\text{in}}\rangle = \otimes_{j=1}^{N} |H\rangle_{m+2j} = |H\rangle_{m+2}|H\rangle_{m+4}\ldots|H\rangle_{m+2N}$, then $|\psi_{\text{out}}\rangle$ reads

$$|\psi_{\text{out}}\rangle = \frac{i^N}{(\sqrt{2})^N} \bigotimes_{j=1}^{N} |L\rangle_{m+2j-1} + \frac{i^N}{(\sqrt{2})^N} \bigotimes_{j=1}^{N} |R\rangle_{m+2j+1} + |\psi_{\text{discard}}\rangle. \quad (7)$$

Here, we use the BS parameter $\Delta = \pi/2$ to maximize the postselection probability. The first two terms in Eq. (7) also superpose an $N$-photon entangled state, which can be postselected by single photon QND of paths $(m+3, m+5, m+2N-1)$ with a success probability of $1/2^{N-1}$.

In the above two cases, the metasurface provides $N$ or $2N$ parallel BS processes with every two adjacent BSs sharing a common output path. When $N = 2$ and 3, the results in Eqs. (6) and (7) are back to our previous discussion. Thus, the parallel BS not only provides a powerful quantum interference ability for multiphoton entanglement generation but also has the potential for high-density quantum integration via improving parallelism in a single metasurface.

### 3.2 Entanglement Fusion

We have shown that the parallel BS metasurface can entangle the previously unentangled photons in a probabilistic way. However, its success probability will decrease quickly as the number of entangled photons increases, which limits the scale of entangled states. The entanglement fusion, which can merge several groups of independent entangled states into a large-scale entangled state,[13] is helpful for performing universal quantum computing.[14] The unique manner of quantum interference in parallel BS makes it possible to realize entanglement fusion and conversion, which will be demonstrated subsequently.

First, consider the fusion and conversion of two pairs of Bell states. The key is to set up the connection between these two entangled pairs. To this end, one of the photons from one pair of the same path passes through the metasurface to interfere with one of the photons from another pair in another path, whereas

another two photons are not involved in the interference process. Here, we use the polarization-entangled state as the resource for fusion, which has the form $|\Psi^+(m)\rangle = (|H\rangle_m|V\rangle_{B,m} + |V\rangle_m|H\rangle_{B,m})/\sqrt{2} = (|L\rangle_m|L\rangle_{B,m} - |R\rangle_m|R\rangle_{B,m})/\sqrt{2}i$, where the subscript $B$ means backward, denoting that the photon is not through the metasurface, and $m$ marks the occupied path mode. As shown in Fig. 5(a), the input state is $|\psi_{\text{in}}\rangle = |\Psi^+(-1)\rangle|\Psi^+(+1)\rangle$. With the transformation $|\psi_{\text{out}}\rangle = \hat{S}(t)|\psi_{\text{in}}\rangle$, the output state reads

$$|\psi_{\text{out}}\rangle = \frac{1}{2}|R\rangle_{+2}|R\rangle_0|L\rangle_{B,-1}|L\rangle_{B,+1} + \frac{1}{2}|L\rangle_{-2}|L\rangle_0|R\rangle_{B,-1}|R\rangle_{B,+1} + |\psi_{\text{discard}}\rangle. \quad (8)$$

Here, $\Delta = \pi/2$ and $|\psi_{\text{discard}}\rangle$ can be discarded through postselection. The first two terms in Eq. (8) have the form of a four-photon entangled state, which means the initial two pairs of Bell states can be fused into a genuine four-photon entangled state with a success probability of 1/2. Note that the postselected state can be changed into a GHZ-type polarization-entangled state if one combines paths $(+2, -2)$ into one single path with a polarizing beam splitter. The entanglement fusion obtained by metasurface originates from four parallel BS processes [red and dark blue arrows in Fig. 5(a)].

The fusion process through a metasurface can also be achieved by destructive detection. It becomes more obvious if we expand the detected photon state on a linearly polarized basis, i.e.

$$\begin{aligned}|\psi_{\text{out}}\rangle = &\frac{1}{2\sqrt{2}}|H\rangle_0|R\rangle_{+2}|L\rangle_{B,-1}|L\rangle_{B,+1} \\ &+ \frac{1}{2\sqrt{2}}|H\rangle_0|L\rangle_{-2}|R\rangle_{B,-1}|R\rangle_{B,+1} \\ &- \frac{i}{2\sqrt{2}}|V\rangle_0|R\rangle_{+2}|L\rangle_{B,-1}|L\rangle_{B,+1} \\ &+ \frac{i}{2\sqrt{2}}|V\rangle_0|L\rangle_{-2}|R\rangle_{B,-1}|R\rangle_{B,+1} + |\psi_{\text{discard}}\rangle. \end{aligned} \quad (9)$$

Now, if only one $H$ (or $V$)-polarized photon is detected in path 0, then we obtain a three-photon entangled state with a success probability of 1/2. In this fusion process, only two sets of BS are involved, so the power of parallel BS is not fully displayed.

Then, the fusion and conversion of three pairs of Bell states are investigated. As shown in Fig. 5(b), only one of the photons from each pair passes through the metasurface, whereas another photon of each pair is propagating backward. If the input state is $|\psi_{\text{in}}\rangle = |\Psi^+(-2)\rangle|\Psi^+(0)\rangle|\Psi^+(+2)\rangle$, as the splitting parameter $\Delta = \pi/2$, the quantum state becomes

$$|\psi_{\text{out}}\rangle = \frac{|R\rangle_{+3}|R\rangle_{-1}|R\rangle_{+1}|L\rangle_{B,-2}|L\rangle_{B,0}|L\rangle_{B,+2}}{2\sqrt{2}} - \frac{|L\rangle_{-3}|L\rangle_{-1}|L\rangle_{+1}|R\rangle_{B,-2}|R\rangle_{B,0}|R\rangle_{B,+2}}{2\sqrt{2}} + |\psi_{\text{discard}}\rangle. \quad (10)$$

The first two terms in Eq. (10) can be postselected by a coincident click of QND single-photon detection in paths

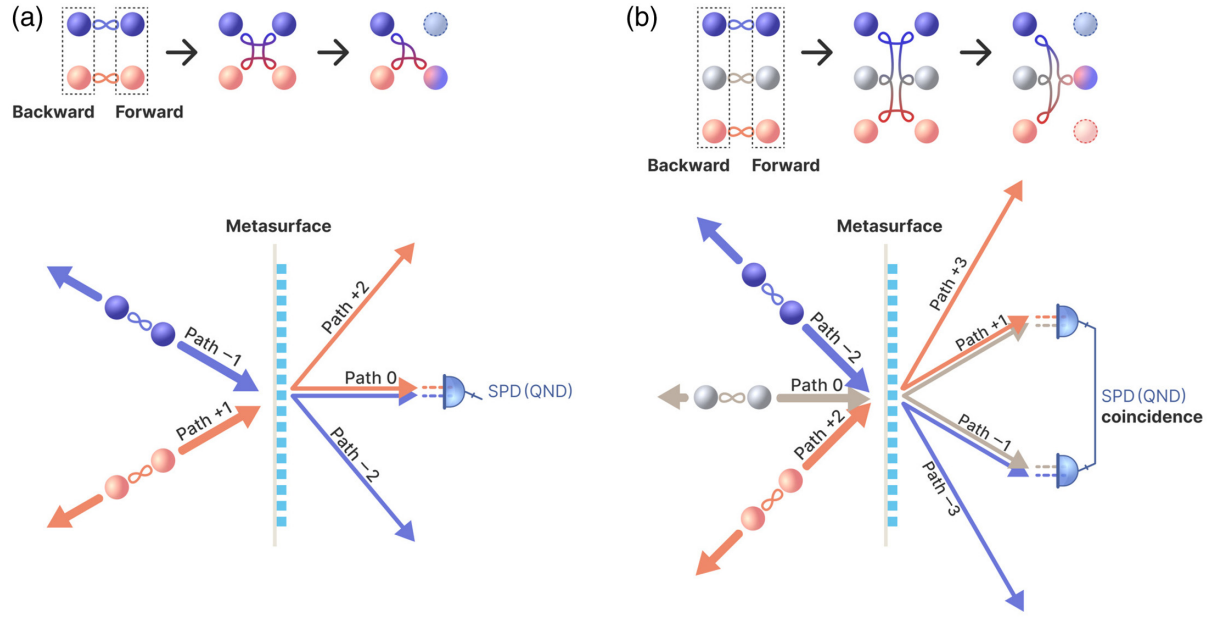


**Fig. 5** Schematic of entanglement fusion and conversion with parallel BS of a metasurface. (a) Fusion and conversion of two pairs of Bell states. (b) Fusion and conversion of three pairs of Bell states. Here, the BS parameter of the metasurface is $\Delta = \pi/2$.

$-1$ and $+1$. They can form a six-photon entangled state with a success probability of 1/4. The fusion of three Bell pairs is achieved through a single gradient metasurface involving six parallel BSs.

By replacing the QND with destructive polarization detection, the fused six-photon entangled state will be converted into a four-photon entangled state. To see this, we change the circular polarization basics into linear ones, and Eq. (10) becomes

$$\begin{aligned}|\psi_{\text{out}}\rangle = {} & |H\rangle_{-1}|H\rangle_{+1}\frac{|R\rangle_{+3}|L\rangle_{B,-2}|L\rangle_{B,0}|L\rangle_{B,+2}-|L\rangle_{-3}|R\rangle_{B,-2}|R\rangle_{B,0}|R\rangle_{B,+2}}{4\sqrt{2}}\\ & -i|H\rangle_{-1}|V\rangle_{+1}\frac{|R\rangle_{+3}|L\rangle_{B,-2}|L\rangle_{B,0}|L\rangle_{B,+2}+|L\rangle_{-3}|R\rangle_{B,-2}|R\rangle_{B,0}|R\rangle_{B,+2}}{4\sqrt{2}}\\ & -i|V\rangle_{-1}|H\rangle_{+1}\frac{|R\rangle_{+3}|L\rangle_{B,-2}|L\rangle_{B,0}|L\rangle_{B,+2}+|L\rangle_{-3}|R\rangle_{B,-2}|R\rangle_{B,0}|R\rangle_{B,+2}}{4\sqrt{2}}\\ & -|V\rangle_{-1}|V\rangle_{+1}\frac{|R\rangle_{+3}|L\rangle_{B,-2}|L\rangle_{B,0}|L\rangle_{B,+2}-|L\rangle_{-3}|R\rangle_{B,-2}|R\rangle_{B,0}|R\rangle_{B,+2}}{4\sqrt{2}}\\ & +|\psi_{\text{discard}}\rangle. \end{aligned} \tag{11}$$

If two $H$-polarized photons in paths $-1$ and $+1$ are simultaneously detected, then the postselected state becomes the first term in Eq. (11), i.e., a four-photon entangled state. Also, the other three possible detection outcomes (HV, VH, and VV) will yield a similar four-photon entangled state. Thus, the fusion of three Bell pairs can be completed in a single metasurface.

The above fusion and conversion scheme can be extended to a more general case with $N$ pairs of Bell states. The input state reads $|\psi_{\text{in}}\rangle = \otimes_{j=1}^{N}|\Psi^{+}(m+2j)\rangle$. When half of the photons pass through the metasurface, the quantum state becomes

$$\begin{aligned}|\psi_{\text{out}}\rangle = {} & \left(\frac{1}{\sqrt{2}}\right)^{N}\bigotimes_{j=1}^{N}|R\rangle_{m+2j+1}|L\rangle_{B,m+2j}\\ & +\left(-\frac{1}{\sqrt{2}}\right)^{N}\bigotimes_{j=1}^{N}|L\rangle_{m+2j-1}|L\rangle_{B,m+2j}+|\psi_{\text{discard}}\rangle. \end{aligned} \tag{12}$$

The first two terms in Eq. (12) can be preserved, which constitutes a $2N$-photon-entangled state. The postselection condition is the same as the situation for $N$-photon-entangled state generation, with a success probability of $1/2^{N-1}$. Here, $2N$ BSs take part in the fusion process. Thus, the parallel BS metasurface provides a compact platform for multipartite entanglement fusion and state conversion.

## 4 Discussion and Conclusion

The parallel BSs of gradient metasurface greatly improve the dimension of entangled states and increase the number of entangled operations. First, multiphoton entanglement can be prepared at a time on a single metasurface. Traditionally, the entanglement dimension increases exponentially as the number of photons increases. Now, it is enabled by the parallel nature of BS in a metasurface. Especially, a larger entanglement dimension can be obtained by increasing the number of available parallel BS processes, which can be realized through enlarging the period of the metasurface without changing its size. This is superior to earlier research on multiphoton entanglement using beam splitters,[9–12] where the number of required beam splitters and photon number increase simultaneously. Second, parallel BS provides a possibility for simultaneous control of several multiphoton entangled states. For example, one can prepare the entanglement on some paths while fusing entanglement on the other paths. As a result, the number of entanglement operations on a single metasurface is increased. This is superior to the previous protocol of entanglement distribution using a multichannel metasurface,[31,32] which is limited to handling only a single entangled state. Therefore, using a single metasurface to fabricate the entanglement meets the demands of high-capacity and multifunctionality in on-chip quantum information processing.

The ability of parallel BS of a single metasurface can be further extended in quantum entanglement. On the one hand, the dimension of the entanglement can be further increased by introducing a new degree of freedom, such as orbital angular momentum.[17] If manipulating $N$ photons at a time, the improvement of entangled state dimension will be greater than those in the previously reported single-photon[27] and two-photon[29] systems. On the other hand, entanglement fusion can occur among multiphoton entangled states in principle, rather than among two-photon entangled states presented here. More importantly, the above extensions and potential applications are all implemented on a single metasurface. Thus, metasurfaces with parallel BS properties can serve as building blocks to achieve denser on-chip quantum integration.

Finally, we briefly discuss the limit of entangled photon number $N$. The limit of $N$ depends on the maximum number of paths supported by parallel BS, which is related to the operating wavelength ($\lambda$), the geometric phase gradient ($k_G$), and the maximum incident angle ($\theta_{\max}$). The parallel BS is valid under the paraxial approximation ($-\theta_{\max} \le \theta \le \theta_{\max}$); then, the angle between two adjacent paths is approximately equal to $\Delta\theta \approx \arcsin[k_G/(2\pi/\lambda)]$. So, the valid path number is estimated as $N \approx 1 + 2\theta_{\max}/\Delta\theta$. It was shown in Ref. 33 that parallel BS is still valid with $\theta_{\max} \approx 15$ deg. Given the current state of the art in micro/nanofabrication technology,[20,28] the range of unit cell period of the metasurface is approximately $p \sim 400$ to 700 nm, whereas the linear phase gradient $k_G = 2\pi/(Mp)$ is built by discretizing $2\pi$ phase with $M$ ($\sim 8-13$) unit cells. For operating wavelength $\lambda = 800$ nm, the maximum number of entangled photons $N$ is expected to reach 3 to 6. Improving fabrication accuracy (larger $M$) and designing metasurfaces that support a wide-angle parallel BS (larger $\theta_{\max}$) will increase $N$.

In summary, we have demonstrated multiphoton entanglement and entanglement fusion through a single gradient metasurface. Based on the multiphoton interference enabled by parallel BS, several kinds of multiphoton entangled states have been prepared from initially unentangled photons. These entangled states have hybrid entanglement features among path-polarization degrees of freedom. Such a parallel BS ability has been further utilized for entanglement fusion to construct a larger-scale entangled state. Hence, the gradient metasurface with parallel BS capability is powerful for controlling multiphoton entanglement. These results pave the way for versatile multiphoton quantum manipulation based on metasurface, which is highly promising for ultracompact quantum devices and multiphoton entanglement sources.

## Acknowledgments

This work was supported by the National Natural Science Foundation of China (Grant Nos. 12474370, 11974032, 12161141010, and T2325022) and the Innovation Program for Quantum Science and Technology (Grant No. 2021ZD0301500).

## References

1. R. Horodecki et al., "Quantum entanglement," *Rev. Mod. Phys.* **81**, 865–942 (2009).
2. J.-W. Pan et al., "Multiphoton entanglement and interferometry," *Rev. Mod. Phys.* **84**, 777–838 (2012).
3. C. Couteau, "Spontaneous parametric down-conversion," *Contemp. Phys.* **59**, 291–304 (2018).
4. L. G. Helt et al., "Spontaneous four-wave mixing in microring resonators," *Opt. Lett.* **35**, 3006–3008 (2010).
5. H.-S. Zhong et al., "12-photon entanglement and scalable scattershot boson sampling with optimal entangled-photon pairs from parametric down-conversion," *Phys. Rev. Lett.* **121**, 250505 (2018).
6. A. Hochrainer et al., "Quantum indistinguishability by path identity and with undetected photons," *Rev. Mod. Phys.* **94**, 025007 (2022).
7. H.-Y. Liu et al., "Deterministic N-photon state generation using lithium niobate on insulator device," *Adv. Photonics Nexus* **2**, 016003 (2022).
8. L.-T. Feng et al., "On-chip quantum interference between the origins of a multi-photon state," *Optica* **10**, 105–109 (2023).
9. Y. L. Lim and A. Beige, "Multiphoton entanglement through a Bell-multiport beam splitter," *Phys. Rev. A* **71**, 062311 (2005).
10. J. Wang et al., "Integrated photonic quantum technologies," *Nat. Photonics* **14**, 273–284 (2020).
11. M. Cherchi et al., "Supporting quantum technologies with an ultralow-loss silicon photonics platform," *Adv. Photonics Nexus* **2**, 024002 (2023).
12. P. Kok et al., "Linear optical quantum computing with photonic qubits," *Rev. Mod. Phys.* **79**, 135–174 (2007).
13. D. E. Browne and T. Rudolph, "Resource-efficient linear optical quantum computation," *Phys. Rev. Lett.* **95**, 010501 (2005).
14. S. Bartolucci et al., "Fusion-based quantum computation," *Nat. Commun.* **14**, 912 (2023).
15. D. Yang et al., "Multiwavelength high-order optical vortex detection and demultiplexing coding using a metasurface," *Adv. Photonics Nexus* **1**, 016005 (2022).
16. H.-T. Chen et al., "A review of metasurfaces: physics and applications," *Rep. Prog. Phys.* **79**, 076401 (2016).
17. A. H. Dorrah and F. Capasso, "Tunable structured light with flat optics," *Science* **376**, eabi6860 (2022).
18. G. Li, S. Zhang, and T. Zentgraf, "Nonlinear photonic metasurfaces," *Nat. Rev. Mater.* **2**, 17010 (2017).
19. Y. Fan et al., "Dual-channel quantum meta-hologram for display," *Adv. Photonics Nexus* **3**, 016011 (2024).
20. X. Li et al., "Simultaneous sorting of arbitrary vector structured beams with spin-multiplexed diffractive metasurfaces," *Adv. Photonics Nexus* **3**, 036010 (2024).
21. L. Li et al., "Metalens-array–based high-dimensional and multiphoton quantum source," *Science* **368**, 1487–1490 (2020).
22. T. Santiago-Cruz et al., "Resonant metasurfaces for generating complex quantum states," *Science* **377**, 991–995 (2022).
23. A. Arbabi et al., "Dielectric metasurfaces for complete control of phase and polarization with subwavelength spatial resolution and high transmission," *Nat. Nanotechnol.* **10**, 937–943 (2015).
24. J. P. Balthasar Mueller et al., "Metasurface polarization optics: independent phase control of arbitrary orthogonal states of polarization," *Phys. Rev. Lett.* **118**, 113901 (2017).
25. X. Zhang et al., "Metasurface-based ultrathin beam splitter with variable split angle and power distribution," *ACS Photonics* **5**, 2997–3002 (2018).
26. Y.-J. Gao et al., "Simultaneous generation of arbitrary assembly of polarization states with geometrical-scaling-induced phase modulation," *Phys. Rev. X* **10**, 031035 (2020).
27. T. Stav et al., "Quantum entanglement of the spin and orbital angular momentum of photons using metamaterials," *Science* **361**, 1101–1104 (2018).
28. P. Georgi et al., "Metasurface interferometry toward quantum sensors," *Light: Sci. Appl.* **8**, 70 (2019).
29. Z.-X. Li et al., "High-dimensional entanglement generation based on a Pancharatnam-Berry phase metasurface," *Photonics Res.* **10**, 2702–2707 (2022).
30. J. Zhang et al., "Single-shot characterization of photon indistinguishability with dielectric metasurfaces," *Optica* **11**, 753–758 (2024).
31. K. Wang et al., "Quantum metasurface for multiphoton interference and state reconstruction," *Science* **361**, 1104–1108 (2018).
32. Y.-J. Gao et al., "Multichannel distribution and transformation of entangled photons with dielectric metasurfaces," *Phys. Rev. Lett.* **129**, 023601 (2022).
33. Q. Liu et al., "Parallel beam splitting based on gradient metasurface: from classical to quantum," *Opt. Express* **32**, 31389–31404 (2024).
34. G. S. Agarwal, *Quantum Optics*, Cambridge University Press (2012).
35. K. Xia, "Quantum non-demolition measurement of photons," in *Photon Counting-Fundamentals and Applications*, N. Britun and A. Nikiforov, Eds., pp. 65–80, InTech (2018).
36. J.-C. Besse et al., "Single-shot quantum nondemolition detection of individual itinerant microwave photons," *Phys. Rev. X* **8**, 021003 (2018).
37. X.-L. Wang et al., "18-Qubit entanglement with six photons' three degrees of freedom," *Phys. Rev. Lett.* **120**, 260502 (2018).

Biographies of the authors are not available.